



HAL
open science

Miniaturized and reconfigurable notch antenna based on a BST ferroelectric thin film

Hung Viet Nguyen, Ratiba Benzerga, Caroline Borderon, Christophe Delaveaud, Ala Sharaiha, Raphael Renoud, Claire Le Paven, Sabrina Pavy, Kevin Nadaud, Hartmut W. Gundel

► To cite this version:

Hung Viet Nguyen, Ratiba Benzerga, Caroline Borderon, Christophe Delaveaud, Ala Sharaiha, et al.. Miniaturized and reconfigurable notch antenna based on a BST ferroelectric thin film. *Materials Research Bulletin*, 2015, 67, pp.255-260. 10.1016/j.materresbull.2015.02.034 . hal-01119380

HAL Id: hal-01119380

<https://hal.science/hal-01119380>

Submitted on 21 May 2015

HAL is a multi-disciplinary open access archive for the deposit and dissemination of scientific research documents, whether they are published or not. The documents may come from teaching and research institutions in France or abroad, or from public or private research centers.

L'archive ouverte pluridisciplinaire **HAL**, est destinée au dépôt et à la diffusion de documents scientifiques de niveau recherche, publiés ou non, émanant des établissements d'enseignement et de recherche français ou étrangers, des laboratoires publics ou privés.

Miniaturized and reconfigurable notch antenna based on a BST ferroelectric thin film

Hung Viet Nguyen^{a,c}, Ratiba Benzerga^{a,*}, Caroline Borderon^b, Christophe Delaveaud^c, Ala Sharaiha^a, Raphael Renoud^b, Claire Le Paven^a, Sabrina Pavy^b, Kevin Nadaud^b, Hartmut W. Gundel^b

^a Institut d'Electronique et de Télécommunications de Rennes (IETR), IUT Saint-Brieuc, Université de Rennes 1, 22004 Saint-Brieuc, France

^b IETR, Université de Nantes, 2 rue de la Houssinière, 44322 Nantes, France

^c CEA-LETI, Minatec, 17 avenue des Martyrs, 38054 Grenoble Cedex 9, France

*Corresponding author. Tel. +332 96 60 96 61, ratiba.benzerga@univ-rennes1.fr

Graphical abstract

Highlights

- A miniature and agile antenna based on a BST MIM capacitor is simulated and made.
- Mn²⁺ doped BST thin films are synthesized by chemical deposition and spin coating.
- Permittivity and losses of the BST thin film are respectively 225 and 0.02 at 1GHz.
- A miniaturization rate of 70 % is obtained with a MIM capacitance of 3.7 pF.
- A frequency tunability of 14.5% and a tunability performance of 0.04 are measured.

ABSTRACT

This work deals with the design, realization and characterization of a miniature and frequency agile antenna based on a ferroelectric Ba_{0,80}Sr_{0,20}TiO₃ thin film. The notch antenna is loaded with a variable Metal/Insulator/Metal (MIM) capacitor and is achieved by a monolithic method. The MIM capacitance is 3.7 pF, which results in a resonant frequency of 670 MHz compared to 2.25 GHz for the unloaded simulated antenna; the resulting

miniaturization rate is 70 %. The characterization of the antenna prototype shows a frequency tunable rate of 14.5 % under an electric field of 375 kV/cm, with a tunability performance $\eta = 0.04$.

Keywords: Oxides; Thin films; Chemical synthesis; Dielectric properties; Ferroelectricity

1. INTRODUCTION

The generalization of communicating systems in the objects of our private and professional life contributes significantly to the development of miniature and agile antennas. The use of a single reconfigurable antenna allows tuning its operating frequency to different communications standards and so, permits replacing multiband antennas in standard devices. This solution offers the possibility to dynamically change the resonance frequency of the antenna through electrical means. The space consumption is greatly reduced for frequency reconfigurable antennas as one single resonant element can be used to cover all the bands. Furthermore, this element is designed for its highest targeted band of operation which results in small size elements. In addition to smaller elements, size reduction in the radio frequency (RF) chain can be achieved by passing some of the filter requirements on a narrow-band antenna design. All these result in space-saving and thus miniaturization.

For the achievement of frequency agile antennas, many solutions have been proposed in literature. The agility of the antenna comes from the modification of its electrical length; it can be obtained, for example, by insertion of active components such as PIN diodes (Positive Intrinsic Negative Diode) [1] or MEMS (Micro-Electro-Mechanical Systems) [2]. The agility can be also obtained by using, as substrate of the antenna, materials with specific properties controlled by an external stimulus (such as an electric or a magnetic field). For that solution, antennas based on meta-materials [3], liquid crystals [4] or ferromagnetic materials (often

ferrites) [5] have been studied. The use of ferroelectric materials, such as KTN ($\text{KTa}_{1-x}\text{Nb}_x\text{O}_3$) [6], BST ($\text{Ba}_{1-x}\text{Sr}_x\text{TiO}_3$) [7], can be envisaged because of the agility of their permittivity under DC electric bias.

In this work, we were interested in an original reconfigurable solution using ferroelectric film, not as substrate of the antenna, but integrated in a localized agile component of the antenna: a MIM (Metal/Insulator/Metal) variable capacitor (varactor) based on a BST ferroelectric thin film. The chosen antenna is an open slot antenna (notch antenna) which shows easy integration in printed circuit and significant miniaturization ratio when loaded with a correctly positioned capacitor [8]. As the operating frequency of the antenna depends on the value of the capacitor load, if this one is variable (by integrating the ferroelectric layer), the antenna may be reconfigurable. The ferroelectric material involved in this study is the perovskite $\text{Ba}_{0,80}\text{Sr}_{0,20}\text{TiO}_3$ compound with a Curie temperature $T_C = 60^\circ\text{C}$ [9]. For this study, it is doped with 1.5%at. of manganese (Mn^{2+}). The Manganese induces the decrease of the oxygen vacancies in the ferroelectric thin film, which allows the reduction of the dielectric losses [10]. Mn^{2+} doped $\text{Ba}_{0,80}\text{Sr}_{0,20}\text{TiO}_3$ films (hereafter noted BST) are produced by chemical solution route and spin-coating deposition [10,11]. Their growth is polycrystalline on stainless steel or alumina substrate [10,12] and their permittivities (ϵ) are in the range [200 - 500] depending on the Mn^{2+} doping level, with dielectric losses less than 0.02 at 1 MHz [10].

The present article is presented as follows: the topology of the studied antenna is first presented along with simulations made by the Ansys HFSS software [13]. The manufacturing of an antenna prototype is further exposed, followed by the characterization of the BST MIM capacitor and the MIM loaded antenna.

2. TOPOLOGY AND SIMULATION OF THE NOTCH ANTENNA BASED ON A BST THIN FILM

Figure 1.a shows the geometry of the studied antenna. The antenna is formed on an alumina substrate of dimension of $25.4 \times 25.4 \text{ mm}^2$ and thickness of 0.508 mm , coated by the BST thin film and metallization layers.

The antenna structure consists of a notch cut from the edge of the ground plane; it is the complementary structure of a conventional quarter wavelength monopole antenna. The notch is etched at the top face of a printed circuit board (PCB) on the substrate. The notch is a rectangular shape slot of width $W = 2 \text{ mm}$ and length $L = 18 \text{ mm}$. For integration and design purposes, the antenna is fed by 50 ohms microstrip line printed on the bottom face. A capacitor, based on a BST thin film, is positioned at the end of the slot. The variation of the permittivity of the BST thin film, by applying a DC bias voltage, allows the modification of the electric length of the slot and so, induces a reconfigurability of the antenna. The detail of the MIM topology is presented in Figure 1.b. For a better trade-off between antenna efficiency and miniaturization rate, low values of capacitance (typically $< 4 \text{ pF}$) have been chosen. For that purpose, the thickness of the BST film and the MIM capacitor area were dimensioned at 1000 nm and $1600 \text{ }\mu\text{m}^2$, respectively. The latter is obtained by the overlapping of the two orthogonal metallic electrodes of 40 microns -width. Two blocking commercial capacitors are used to decouple the RF signal of the antenna to the applied electric DC voltage; their capacitance is 56 pF .

This specific design was simulated under the Ansys HFSS software in order to validate the chosen antenna topology. Simulations were performed with the following dimensions (Figure 1.a): W (slot width) = 2 mm ; L (slot length) = 18 mm ; L_f (length of the microstrip line) = 7 mm ; a (power line position) = 8 mm .

To simulate the agility of the antenna, different values of the BST permittivity (from 250 to 150) were taken into account. These permittivities are those obtained under the applying of a DC electric field in our previous work on a $\text{Ba}_{0,80}\text{Sr}_{0,20}\text{TiO}_3$ thin film doped with 1.5% of

Mn^{2+} [10]; corresponding dielectric losses were measured between 0.008 and 0.015 [10]. Here, to simplify simulation calculations, we assume constant losses equal to 0.02, greater than the previously maximum measured value. The variation of ϵ corresponds to a permittivity agility $A = 40\%$. The agility A is defined using the following relation:

$$A = \left| \frac{\epsilon_{\max} - \epsilon_{\min}}{\epsilon_{\max}} \right| \quad (\text{Eq. 1})$$

where ϵ_{\max} and ϵ_{\min} are the maximum and minimum values of the permittivity of the BST film.

Figure 2 shows the simulated S_{11} reflection parameter of the antenna as a function of the frequency. A shift of the resonant frequency from 640 MHz to 800 MHz is obtained when ϵ decreases and corresponds to an antenna frequency tunable rate TR of 22%. TR is calculated by:

$$TR = \left| \frac{f(\epsilon_{\min}) - f(\epsilon_{\max})}{[f(\epsilon_{\min}) + f(\epsilon_{\max})]/2} \right| \quad (\text{Eq. 2})$$

where $f(\epsilon_{\min})$ and $f(\epsilon_{\max})$ are the resonant frequencies of the antenna with, respectively, minimum and maximum permittivity values of the BST film.

Given that the resonant frequency of the simulated antenna without BST MIM capacitor is 2.25 GHz, a miniaturization rate MR of 71% is obtained on the size of the antenna. The miniaturization rate is defined as:

$$MR = \left| \frac{f_{\text{Loaded}} - f_{\text{Unloaded}}}{f_{\text{Unloaded}}} \right| \quad (\text{Eq. 3})$$

where f_{Loaded} is the resonant frequency of a MIM capacitor loaded antenna and f_{Unloaded} is the resonant frequency of unloaded antenna.

3. IMPLEMENTATION OF THE NOTCH ANTENNA PROTOTYPE BASED ON A BST THIN FILM

A monolithic implementation of the antenna prototype was performed. The variable MIM structure capacitor based on the ferroelectric BST thin film was formed on the alumina substrate by successive deposition of the lower electrode, the BST layer and the upper electrode.

The lower electrode, made of 200 nm-thick layer of platinum, was first deposited. This deposition was achieved through a mechanical mask by radio frequency (RF) magnetron sputtering. The deposition of the Mn^{2+} doped $\text{Ba}_{0,80}\text{Sr}_{0,20}\text{TiO}_3$ film was subsequently made by chemical solution technique. The precursor solution was composed of barium and strontium acetates to which a titanium n-propoxide and an organic stabilizer were mixed in appropriate proportions. Details of the deposition parameters are summarized in [10,11]. The solution was deposited on the substrate by spin-coating. A heat treatment at 750 °C allows the evaporation of the organic material and the crystallization of the BST film in the ferroelectric perovskite structure. Several steps "deposit by spin coating + heat treatment" were repeated to obtain the required final BST film thickness. The BST thin film covers the entire surface of the substrate.

Before the deposition of the upper electrode, the via connection to the lower electrode was created by chemical etching of the BST layer [14]. The deposition of the top copper electrode (1 micron thick), performed by RF-sputtering through a mechanical mask, completes the geometry of the MIM varactor. The bottom electrode of this varactor is directly connected to the upper edge of the slot, hence directly connected to the ground plane. The upper electrode is connected to the small metallic patch P , and thus, the BST capacitor is formed. The RF signal is coupled by 2 DC blocking capacitors of 56 pF. For DC voltage applying, one electrode of the DC source is connected to the ground plane; the other is connected to the

small metallic patch P (Figure 1.a).

The loaded antenna prototype is shown in Figure 1.c. The ground plane of the antenna has been expanded to facilitate its connection to the characterization device and also to improve the antenna performance.

4. CHARACTERIZATION

4.1. BST CAPACITOR

The characterization in low frequencies of the MIM capacitor based on the BST film was realized on an Agilent 4294A impedance-meter before the addition of the DC blocking capacitors. It gives a capacitance value of 3.8 pF and dielectric losses $\tan\delta = 0.02$ at 1 MHz. Figure 3 shows the change of the capacitance as a function of the applied DC bias voltage. A variation of the capacitance from 3.8 pF to 2.1 pF is observed when the DC voltage increases from 0 V to 40 V (at 1 MHz); this corresponds to a permittivity agility $A = 45\%$ (Eq. 1). The rapid decline of the permittivity beyond 1 MHz and the discontinuity of the curves (after 8 MHz) are artificial and are due to the frequency limitation of the measurement technique. Capacitance values in high frequencies are thus obtained by extrapolating the curves plotted in low frequencies, as can be seen in Figure 3. At 1 GHz, the capacitance is estimated at 3.7 pF. Considering the actual dimensions of the MIM structure (surface of $1500\ \mu\text{m}^2$ and a BST film thickness of 800 nm), a permittivity value of 225 is calculated for the deposited thin film. At 1 GHz, the permittivity agility has been estimated at 40% for a DC bias voltage of 40 V and at 35% for a DC bias voltage of 30 V. These values are very close to those used in simulations.

4.2. ANTENNA PROTOTYPE CHARACTERIZATION

The measured reflection coefficient of the antenna as a function of applied DC voltage is

presented in Figure 4. The measurement was performed using a vector network analyzer (VNA Rohde Schwarz, working frequency range 0-24 GHz). The DC bias voltage was controlled by a DC generator (QL 355 TTI, max voltage of 35 V). Figure 4 shows that the resonant frequency of the antenna prototype shifts from 670 MHz to 774 MHz under the application of a DC voltage varying from 0 to 30 V. This corresponds to a frequency tunable rate TR of 14.5 % (Eq. 2). Considering the resonant frequencies of the BST loaded antenna prototype (670 MHz) and the unloaded simulated antenna (2.25 GHz), the experimental miniaturization rate is $MR = 70$ % (Eq. 3).

A retro-simulation of the antenna prototype response was performed by Ansys HFSS software considering the real dimensions of the prototype and taking into account the presence of the measuring cable. The matching of the retro-simulated resonant frequency to the experimental one (Figure 5) was achieved by permittivity values of 220 (at 0 V) and 160 (at 30 V). These retro-simulated values are in agreement with the value of 225 obtained at 0 V and 1 GHz by extrapolation of measurements.

3D gain patterns of the antenna prototype were obtained by measuring the antenna in an anechoic chamber (see supplementary data). As shown before in Figure 4, when the applied voltage increased from 0 V to 30 V, the resonant frequency shifted from 670 MHz to 774 MHz. Ideally, the gain antenna measurements should cover both of these two frequencies; however, the frequency limit of the instruments used during this characterization had imposed measurements above 700 MHz. Gain patterns allow the calculation of the radiation efficiency of the prototype for DC bias voltage of 0 and 30 V, as observed in Figure 6. Figure 6.a shows that the maximum radiation efficiency of the antenna is weak. This low level is mainly explained by the miniaturization of the antenna, with very small electrical dimensions ($\lambda_0/28$ for the slot and $\lambda_0/11 \times \lambda_0/7 \times \lambda_0/900$ for the ground plane at 700 MHz). Moreover, a large difference is observed between the measurement and simulation. This is probably due to

higher experimental losses than those simulated, introduced by the different materials constituting the antenna prototype.

In Figure 6.b, one can observe that the radiation efficiency of the antenna increases with the applied DC bias voltage. This can be explained by the fact that the permittivity of the ferroelectric film decreases as the voltage increases, so that the operating point of the antenna moves towards higher frequencies when loaded and the antenna appears electrically larger. Consequently, an increase in gain is obtained, which induces an increase in radiation efficiency. This is coherent with the fundamental laws of miniature antennas [15].

A study of the potential sources of losses responsible for the low antenna efficiency has been carried out by simulation. Two effects have been studied: first, the thickness of the copper metallization and thereafter, the BST dielectric loss. For the first study, the copper metallization has been increased from 1 micron to 200 microns (Figure 7.a), maintaining fixed dielectric properties of the BST layer ($\tan\delta = 0.02$ and $\varepsilon = 160$, obtained by retro-simulation of the BST loaded antenna measurement under DC voltage of 30 V). For the second study, the BST thin film was simulated with dielectric loss $\tan\delta$ decreasing from 0.05 to 0.001 (Figure 7.b), keeping the BST thickness equal to 1 μm .

First graph shows that the radiation antenna efficiency is improved when the thickness of the metallization is increased, which is explained by the corresponding reduction of losses introduced by the skin effect. Above 5 microns of metallization (which corresponds to 2 times the skin thickness at the frequency of 670 MHz) [16], the efficiency converges towards that of a Perfect Electric Conductor (PEC), which theoretically does not possess losses. Figure 7.b shows that the radiation efficiency of the antenna is strongly increased when the dielectric losses of the BST material are decreased. With BST losses of 0.001, the efficiency is more than 20 % for frequencies higher than 670 MHz. The efficiency is far higher (60 %) around 800 MHz, which confirm that a trade-off between efficiency and miniaturization has

to be taken into account in the design of miniaturized antennas.

To quantify the efficiency of the antenna frequency agility, a tunability performance (η) is defined as:

$$\eta = \frac{TR}{E_{\max} - E_{\min}} \quad (\text{Eq. 4})$$

where E_{\max} and E_{\min} (kV/cm) are the electric bias fields used for the tuning control of the BST thin film and TR is the antenna frequency tunable rate (here, the maximum voltage is 30 V, which corresponds to a maximum electric field of 375 kV/cm).

The calculated η is 0.04. This is the best performance reported up to now in the literature (for example, $\eta = 0.03$ in [17]) for a technology incorporating ferroelectric thin films in planar antennas. As mentioned before, higher performances could be obtained by increasing the metallization thickness but also by improving the BST thin film dielectric losses.

5. CONCLUSION

In this work, a slot antenna, loaded with a tunable ferroelectric charge capacitor based on a Mn^{2+} doped $\text{Ba}_{0,80}\text{Sr}_{0,20}\text{TiO}_3$ thin film, was studied. The manufacturing of a prototype was performed by monolithic method and validates the antenna design. The agility of the permittivity of the BST ferroelectric thin film was extrapolated at about 35 % at 1 GHz for a maximum electric field of 375 kV/cm. This induces an antenna frequency tunable rate of 14.5 %, corresponding to a tunability performance of 0.04. The loaded antenna prototype, compared to the simulated antenna without the MIM structure and ferroelectric thin film, has a degree of miniaturization of 70 %.

6. ACKNOWLEDGEMENTS:

The authors want to thank CEA Leti and CNRS for their financial supports and Cooksonelectronics Cholet for achieving the mechanical masks used during the electrodes deposition.

REFERENCES

- [1] J. -M. Laheurte, Switchable CPW-fed slot antenna for multifrequency operation, *Electron. Lett.* 37 (2001) 1498–1500.
- [2] Z. Liu, K. Boyle, Joonas Krogerus, M. de Jongh, K. Reimann, R. Kaunisto, and J. Ollikainen, MEMS-Switched, Frequency-Tunable Hybrid Slot/PIFA Antenna, *IEEE Antennas Wireless Propag. Lett.* 8 (2009) 311–314.
- [3] M. A. Abdalla and Z. Hu, Compact and tunable metamaterial antenna for multi-band wireless communication applications, *IEEE International Symposium on Antennas and Propagation* (2011) 1054–1057.
- [4] S. Missaoui, M. Kaddour, and A. Gharbi, Design and simulation reconfigurable liquid crystal patch antennas on foam substrate, *J. Chem. Eng. Mater. Sci.* 2 (2011) 96–102.
- [5] R. K. Mishra, S. S. Pattnaik, and N. Das, Tuning of microstrip antenna on ferrite substrate, *IEEE Trans. Antennas Propag.* 41 (1993) 230–233.
- [6] Q. Simon, Y. Corredores, X. Castel, R. Benzerga, R. Sauleau, k. Mahdjoubi, A. Le Febvrier, S. Deputier, M. Guilloux-viry, L. Zhang, P. Laurent, G. Tanne, Highly tunable microwave stub resonator on ferroelectric $\text{KTa}_{0.5}\text{Nb}_{0.5}\text{O}_3$ thin film, *Appl. Phys. Lett.* 99 (2011) 092904-1/3.
- [7] L. C. Sengupta, S. Sengupta, Breakthrough advances in low loss tunable dielectric

materials, *Mater. Res. Innov.* 2 (1999) 278-282.

[8] C. Lach, L. Rudant, C. Delaveaud, A. Azoulay, A new miniaturized antenna for ISM 433 MHz frequency band, *Proceeding of European Conference on Antennas and Propagation (EuCAP)*, Barcelona, Spain (2010) 1-5.

[9] B. A. Baumert, L. H. Chang, A. T. Matsuda T. L. Tsai, C. J. Tracy, R. B. Gregory, P. L. Fejes, N. G. Cave, W. Chen, D. J. Taylor, T. Otsuki, E. Fujii, and S. Hayashi, K. Suu, Characterization of sputtered barium strontium titanate and strontium titanate-thin films, *J. Appl. Phys.* 82 (1997) 2558-2566.

[10] K. Nadaud, C. Borderon, S. Pavy, H.W. Gundel, Realization and characterization of manganese doped BST thin films for reflectarray applications, *Proceeding of IEEE International Symposium on the Applications of Ferroelectric and Workshop on the Piezoresponse Force Microscopy (ISAF/PFM)*, (2013) 145-148.

[11] C. Borderon, D. Averty, R. Seveno, and H. W. Gundel, Preparation and Characterization of Barium Strontium Titanate Thin Films by Chemical Solution Deposition, *Ferroelectrics* 362 (2008) 1–7.

[12] C. Borderon, D. Averty, R. Seveno, H. W. Gundel, Influence of the Morphology of Barium Strontium Titanate Thin Films on the Ferroelectric and Dielectric Properties, *Integr. Ferroelectr.* 93 (2007) 133–140.

[13] Ansys, Ansys HFSS. 2012.

[14] S. Pavy, S. Baron, C. Borderon, and H. W. Gundel, Wet chemical etching of BaSrTiO₃ ferroelectric thin films, *Proc. International Symposium on Intergated Functionalities*, Cambridge, England, (2011).

- [15] L. J. Chu, Physical Limitations of Omni-Directional Antennas, *J. Appl. Phys.* 19 (1948) 1163–1175.
- [16] E.C. Jordan, K. G. Balmain, *Electromagnetic Waves and Radiating Systems*, 2nd edition 1968, Prentice Hall, Chapter 5 (1968).
- [17] H. Jiang, M. Patterson, D. Brown, C. Zhang, K. Pan, G. Subramanyam, D. Kuhl, K. Leedy, and C. Cerny, Miniaturized and Reconfigurable CPW Square-Ring Slot Antenna Loaded With Ferroelectric BST Thin Film Varactors, *IEEE Trans. Antennas Propag.* 60, (2012) 3111 –3119.

List of figure captions

Figure 1: a) Scheme of the notch antenna b) details of the varactor based on a BST thin film and c) Photo of the notch antenna prototype loaded with a MIM varactor based on a BST thin film

Figure 2: Variation of the reflection parameter (S_{11}) of the notch antenna according to the permittivity of the BST thin film compared to an antenna without a BST MIM capacitor

Figure3: Evolution of the MIM capacitance based on the BST film as a function of the DC voltage (with the extrapolation at 1 GHz)

Figure 4: Reflection parameter (S_{11}) of the notch antenna prototype loaded by a BST varactor

Figure 5: Measurement vs retro simulation of the reflection parameter (S_{11}) of a notch antenna loaded by a BST varactor

Figure 6: Measurement vs retro-simulation of the radiation efficiency of a notch antenna loaded by a BST varactor under DC voltage of a) 0V and b) 30V

Figure 7: Simulated radiated efficiency of a notch antenna loaded by a BST varactor as a function of frequency for a) different metallic thickness and b) different BST dielectric losses

Figure 1

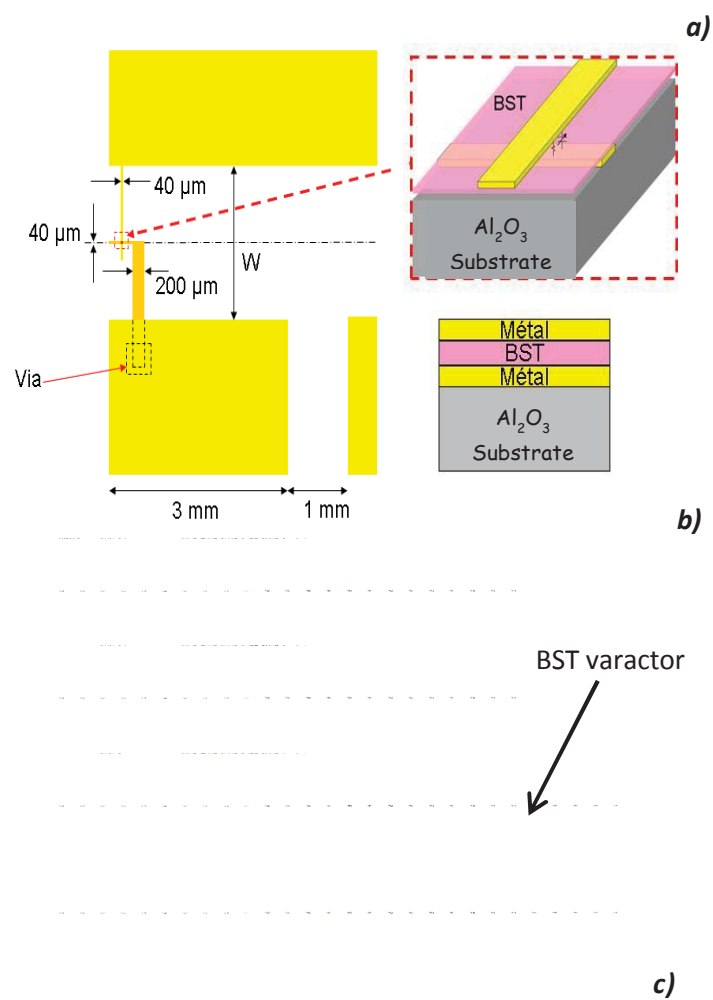


Figure 2

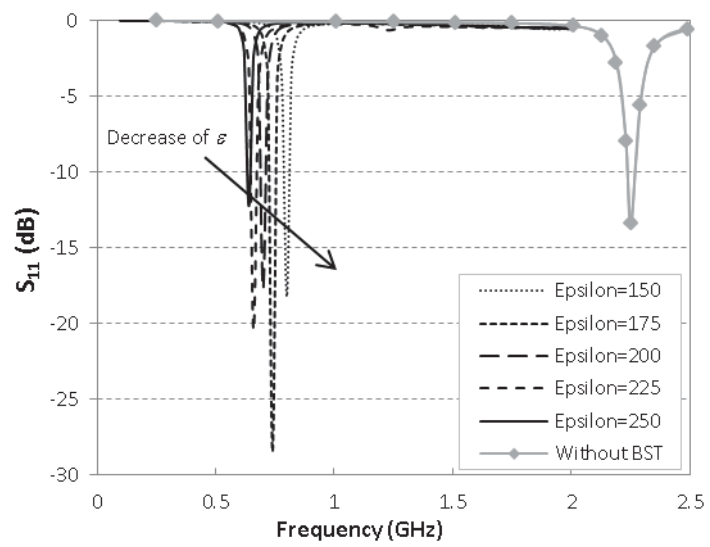


Figure 3

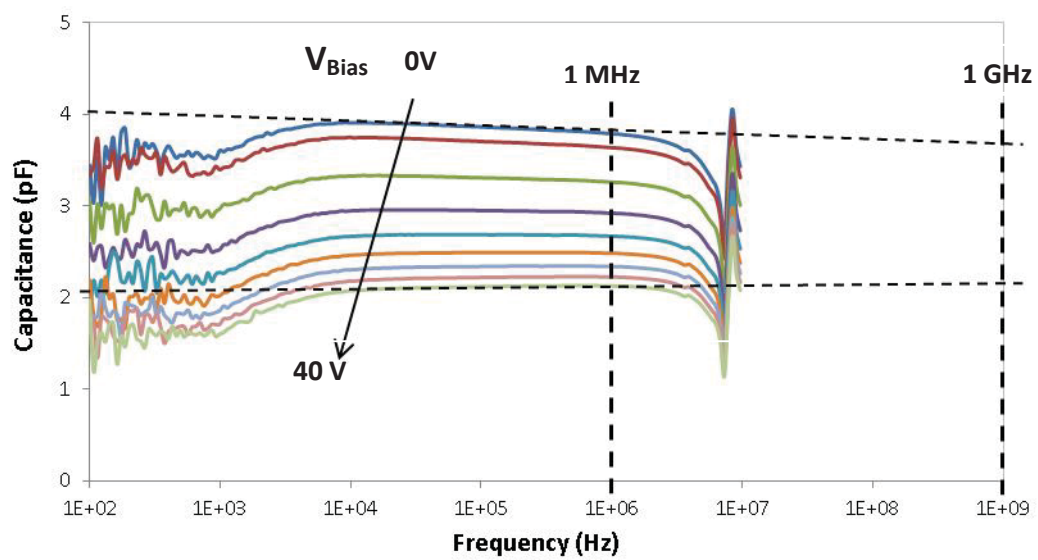


Figure 4

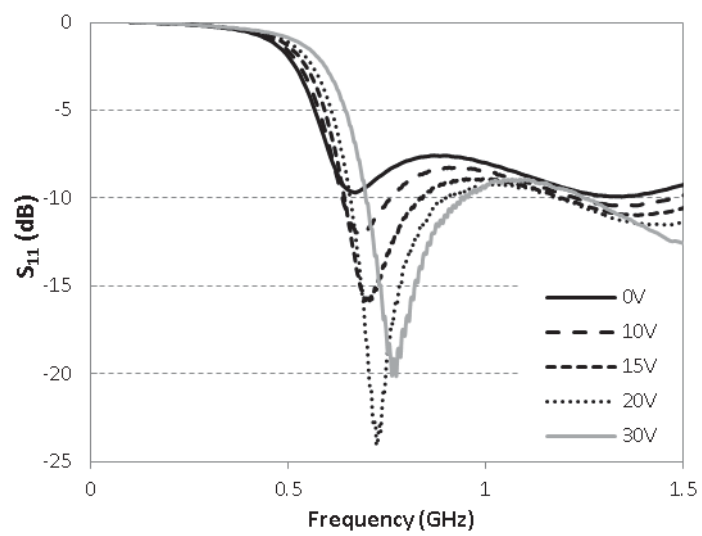


Figure 5

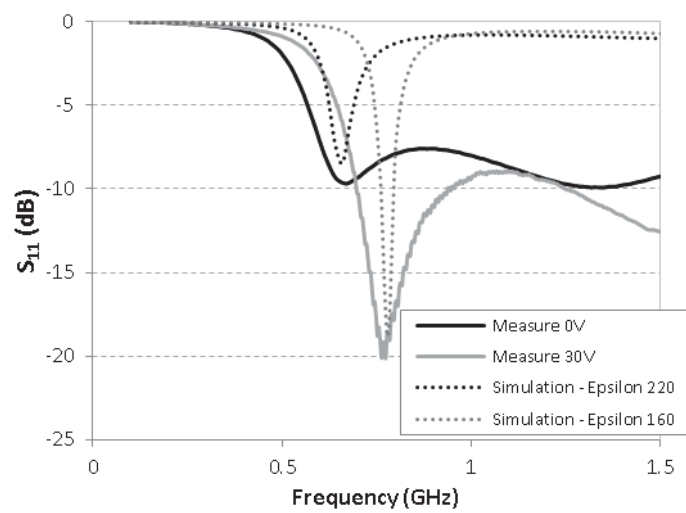


Figure 6

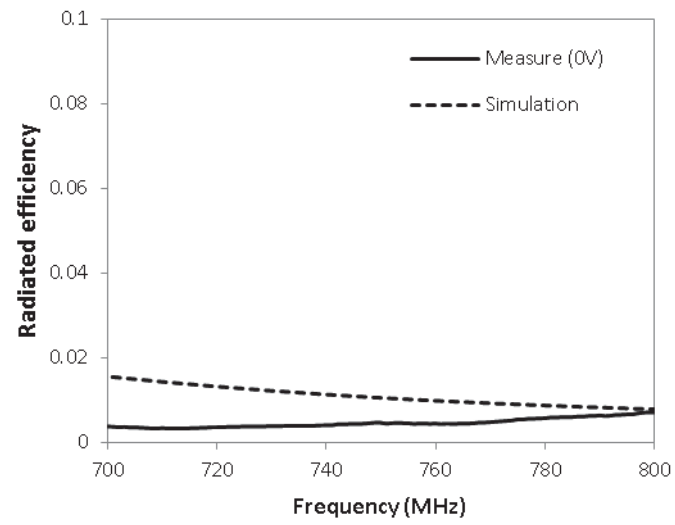
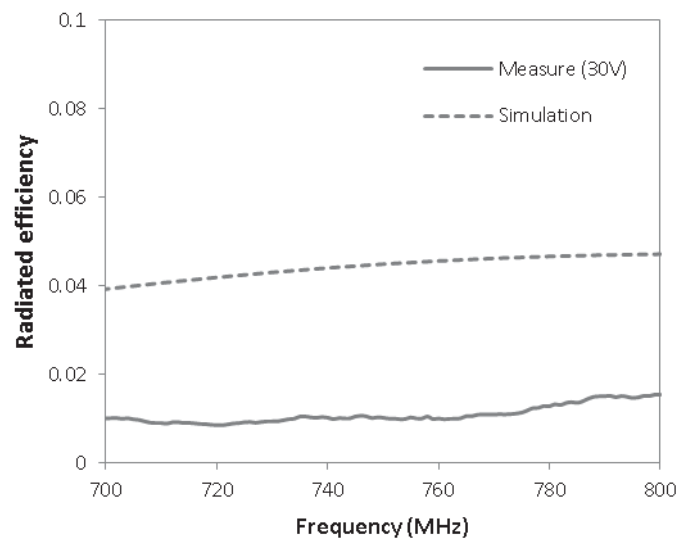
*a)**b)*

Figure 7

